Organic & Biomolecular Chemistry

ROYAL SOCIETY OF CHEMISTRY

PAPER

Published on 10 July 2026

Cite this: *Org. Biomol. Chem.*, 2026, **24**, 6082

Toward a sustainable protection group approach for solid-phase oligonucleotide synthesis employing 5′-*O*-(2-methoxyisopropyl) protection

Verneri Saari,[a] Mikko Ora,[a] Alejandro Gimenez Molina,[b] Andras Horvath,[b] Yogesh S. Sanghvi[c] and Pasi Virta *[a]

Received 3rd June 2026,
Accepted 10th July 2026

DOI: 10.1039/d6ob00858e

rsc.li/obc

5′-*O*-(2-Methoxyisopropyl) (MIP)-protected nucleoside-3′-*O*-phosphoramidites were synthesized and evaluated as novel building blocks for automated solid-phase oligonucleotide synthesis (SPOS). Activators and additives were screened to establish the optimal conditions for the coupling of the 5′-*O*-MIP building blocks. Approximately half the amount of the deblocking reagent can be used to remove 5′-*O*-MIP compared to 5′-*O*-4,4′-dimethoxytrityl (DMT) with twice the rate for its deprotection. The faster 5′-*O*-deprotection rate reduced overall acid consumption, while the small-molecule benign byproducts (acetone and methanol) generated *via* MIP deprotection permit a lower PMI during SPOS. This work potentially leverages the improved design of sustainable strategies for the manufacturing of therapeutic oligonucleotides.

Introduction

Automated solid-phase oligonucleotide synthesis (SPOS), utilizing 5′-*O*-4,4′-dimethoxytrityl (DMT)-protected nucleoside monomers and the phosphoramidite coupling chemistry, has been the predominant technology for the preparation of oligonucleotides over four decades.[1] This method offers excellent reproducibility and a high-yielding synthesis cycle, which results in fast chain elongation of oligonucleotide sequences on demand. The chemistry of the DMT protecting group plays a vital role in successful SPOS. It can orthogonally and rapidly be removed by mild acid treatment (1–10% di- or trichloroacetic acid in dichloromethane or toluene). In addition, the colorimetric detection of the released DMT cation can be used to determine the coupling efficiency of the monomers and to minimize the acid exposure needed for complete detritylation.[2] However, the detritylation step accounts for a significant part, about 21%, of the process mass intensity (PMI) of the entire SPOS workflow.[3] The overall acid exposure of the synthesis may also result in partial depurination of purine-rich 2′-deoxyribonucleotide (DNA) sequences. Furthermore, the DMT group corresponds to approximately 35% of the total mass of phosphoramidite monomers, leading to poor atom economy of the synthesis.[4,5] Therefore, replacing DMT with lower-molecular-weight and more acid-labile or alternatively removable 5′-*O*-protecting groups could be investigated to improve atom economy and reduce reagents and solvent consumption, ultimately lowering the PMI of SPOS. Structural analogues of trityl, 9-phenylxanthen-9-yl (pixyl),[6–10] silyl,[11–13] acyl,[14] carbonate,[15,16] and photosensitive groups[17–20] have been used as 5′-*O*-protecting groups for special purposes, but DMT is still the 5′-*O*-protecting group of choice during conventional SPOS.[21,22]

Additionally, 5′-*O*-(2-methoxyisopropyl) (MIP)-protected nucleosides, including phosphoramidites[23–25] and limonene-derived P(v)-building blocks,[26] have been used in liquid-phase oligonucleotide synthesis (LPOS) (Fig. 1A). MIP is a relatively small protecting group (molecular weight of MIP *vs.* DMT: 73

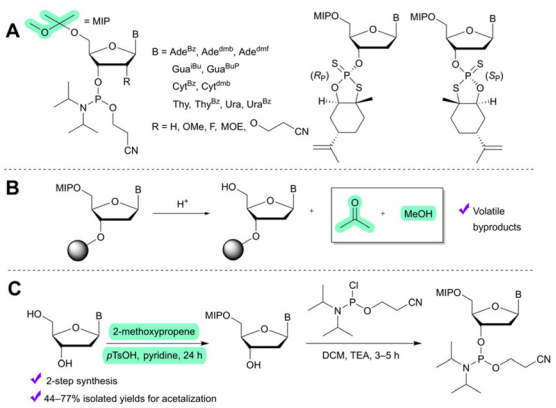

Fig. 1 (A) 5′-*O*-MIP-protected building blocks used in liquid-phase oligonucleotide synthesis (LPOS). (B) Removal of the MIP group yields volatile byproducts acetone and methanol. (C) Selective 5′-*O*-acetalization of nucleosides in pyridine followed by standard phosphitylation.

[a]*Department of Chemistry, University of Turku, 20500 Turku, Finland. E-mail: pamavi@utu.fi*
[b]*Janssen Pharmaceutica N.V., 30 Turnhoutseweg, B-2340 Beerse, Belgium*
[c]*Rasayan Inc., 2802 Crystal Ridge Road, Encinitas, CA 92024-6615, USA*

vs. 303 g mol^{-1}). Under hydrolytic conditions, it undergoes *ca.* 4.5-fold faster acid-catalyzed cleavage than the DMT group.[27,28] Its irreversible deprotection mechanism, resulting in the volatile byproducts acetone and methanol (Fig. 1B),[29] facilitates the isolation and purification of the growing oligonucleotides in LPOS. Recently, a selective 5′-*O*-acetalization method was developed (Fig. 1C), which further increased the value of 5′-*O*-MIP-protected building blocks as potential substitutes for DMT-protected analogs.[30] The 5′-*O*-MIP building blocks are free-flowing solid compounds as amidites at room temperature and are stable in acetonitrile, making their handling similar to that of the DMT analogs.

In this study, for the first time, MIP was evaluated as an alternative 5′-hydroxyl protecting group for automated SPOS. The acid sensitivity makes MIP susceptible to premature cleavage under slightly acidic conditions of the phosphoramidite coupling. This has not been a serious issue in batch reactions of LPOS, wherein nearly stoichiometric amounts of activators are used for the assembly of relatively short oligonucleotide sequences.[23–25,27] The continuous-flow system with an excess of activators in SPOS, however, is a more challenging environment considering the lability of MIP. The possibility of premature MIP cleavage during the coupling step in the presence of an acidic activator may result in the formation of n + 1 side products, the relative amount of which increases when the total coupling time of the synthesis increases (correlating with the length of the target sequence). Therefore, different activators in the presence and absence of mild bases were carefully screened to find the optimal conditions for coupling the 5′-*O*-MIP building blocks. A comparative analysis was performed to show a faster deblocking time with the 5′-*O*-MIP *vs.* DMT-protected nucleosides. Finally, a therapeutically relevant phosphorothioate oligonucleotide (fomivirsen) was assembled under the optimized conditions to demonstrate the feasibility of using 5′-*O*-MIP protection in SPOS.

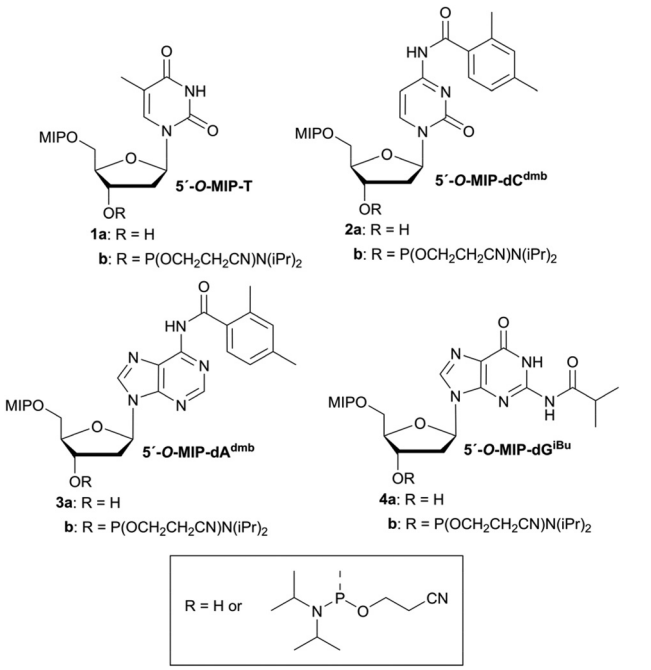

Fig. 2 5′-*O*-MIP-protected nucleosides **1a–4a** (R = H) and the corresponding phosphoramidite building blocks **1b–4b** (R = P(OCH$_2$CH$_2$CN)N(iPr)$_2$) examined in the present study.

Results and discussion

Stability of 5′-*O*-MIP under coupling conditions

Prior to the SPOS experiments, the stability of 5′-*O*-MIP-protected nucleosides (**1a–4a**, Fig. 2) was examined in various coupling cocktails, including 5-benzylthio-1*H*-tetrazole (BTT, pK_a 4.1), 1*H*-tetrazole (pK_a 4.9), 4,5-dicyanoimidazole (DCI, pK_a 5.2), and pyridinium trifluoroacetate (PTFA, pK_a 5.3) combined with *N*-methylimidazole (NMI, pK_a 7.0)[31] in the presence of 2 equiv. of methanol (Table 1). Acetonitrile was selected as the main solvent for the experiments, and dimethylformamide was added to the mixtures to improve the solubility of the nucleosides. The reaction mixtures were monitored by reversed-phase HPLC analysis. The stability of 5′-*O*-MIP-T (**1a**) was first examined. After 24 h of incubation with a stoichiometric amount of the activators, the 5′-*O*-MIP group appeared to be the most stable (97%) in a mixture of 1*H*-tetrazole (entry 2) and the least stable (6%) in a mixture of PTFA/NMI combination (entry 4) (Table 1). Approximately equal stability (56 and 59%) was observed in the mixtures of BTT and DCI (entries 1 and 3). Based on the obtained data, the aqueous pK_a values of the activators do not predict the cleavage rate of MIP. The trend of the results is similar to that observed for the 5′-*O*-(2-isopropoxyprop-yl) protecting group.[27] The counterion of the mild acid in organic solvents potentially affects the deprotection rate, which does not correlate with the aqueous pK_a values of the activators. These observations narrowed down the possible activators.

Systems containing 1*H*-tetrazole or BTT were next examined in more detail. The synthesizer used in this study (ÄKTA OligoPilot™ Plus 10) mixes the phosphoramidite building block (0.1 mol L^{-1} in acetonitrile; 15 equiv./5′-OH group in 1 μmol scale synthesis) and a commercial ready-made activator solution (*e.g.*, 0.45 mol L^{-1} 1*H*-tetrazole or 0.30 mol L^{-1} BTT in acetonitrile) at a 2 : 3 (v/v) ratio and recycles this combined cocktail through the column at a 4.5 mL min^{-1} flow rate. The final concentrations of the phosphoramidite building block (0.04 mol L^{-1}) and the activator (0.18 mol L^{-1} BTT or 0.27 mol L^{-1} 1*H*-tetrazole) correspond to 4.5 equiv. of BTT or 6.8 equiv. of 1*H*-tetrazole compared to the building block. Prior to the delivery of the reagents, the synthesis column and tubing contain acetonitrile (<1 mL), which dilutes the coupling cocktail. This means that the initial concentrations of the reagents reduce, but the initial equivalents of the reagents remain unchanged in the eventual coupling reaction. After 24 h of incubation under these conditions (entries 5–9), substantial MIP cleavage (23% and 68% in 1*H*-tetrazole and BTT solutions, respectively) was observed. Pyridine (pK_a 5.3) can be added to

Table 1 Stability of 5′-*O*-MIP- and 5′-*O*-DMT-protected nucleosides under different coupling, oxidation, and sulfurization conditions. The reported equivalents are in relation to the nucleoside. In all of the reactions, two equivalents of methanol are used. See the exact reaction and chromatographic conditions in the Experimental section

Entry	Time	Nucleoside conc. (mol L^{-1})	Reagent (mol L^{-1})	Solvent system (v/v)	Base (equiv.)	**1a** (%)	5′-*O*-DMT-T (%)	**2a** (%)	**3a** (%)	**4a** (%)
1	24 h	0.11	BTT (0.11)	ACN–DMF, 1 : 1	n.a.	56	99	n.a.	n.a.	n.a.
2	24 h	0.11	1*H*-Tetrazole (0.11)	ACN–DMF, 1 : 1	n.a.	97	99	n.a.	n.a.	n.a.
3	24 h	0.11	DCI (0.11)	ACN–DMF, 1 : 1	n.a.	59	98	n.a.	n.a.	n.a.
4	24 h	0.11	PTFA (0.11) + NMI (0.05)	ACN–DMF, 1 : 1	n.a.	6	94	n.a.	n.a.	n.a.
5	24 h	0.04	BTT (0.18)	ACN–DMF, 9 : 1	n.a.	32	97	n.a.	n.a.	n.a.
6	24 h	0.04	1*H*-Tetrazole (0.27)	ACN–DMF, 9 : 1	n.a.	77	98	n.a.	n.a.	n.a.
7	24 h	0.04	BTT (0.18)	ACN–DMF–pyridine, 41 : 5 : 4	Pyridine (25)	49	97	n.a.	n.a.	n.a.
8	24 h	0.04	BTT (0.18)	ACN–pyridine, 3 : 2	Pyridine (125)	82	98	n.a.	n.a.	n.a.
9	24 h	0.04	BTT (0.18)	ACN–DMF–lutidine, 41 : 5 : 4	Lutidine (17)	78	99	n.a.	n.a.	n.a.
10	30 min	0.04	BTT (0.18)	ACN–DMF–pyridine, 41 : 5 : 4	Pyridine (25)	98	n.a.	98	95	95
11	60 min	0.04	BTT (0.18)	ACN–DMF–pyridine, 41 : 5 : 4	Pyridine (25)	96	n.a.	97	88	90
12	24 h	0.06	I_2 oxidizer (0.05)	H_2O–pyridine, 1 : 9	n.a.	82	100	n.a.	n.a.	n.a.
13	24 h	0.05	CSO oxidizer (0.42)	ACN–DMF, 5 : 1	n.a.	10	10	n.a.	n.a.	n.a.
14	24 h	0.05	PolyOrg Sulfa (0.08)	ACN–DMF, 5 : 1	n.a.	100	100	n.a.	n.a.	n.a.

n.a. = not available.

the coupling cocktails to lower the acid potential of the activators while still maintaining sufficient acid-catalyzed activation of the phosphoramidites.[32] 5′-*O*-MIP-T (**1a**) was next exposed to mixtures of BTT (0.18 mol L^{-1}) in the presence of pyridine (25 and 125 equiv./nucleoside, for the rationale behind these equivalents, *cf.* the SPOS experiments below) or 2,6-lutidine (17 equiv./nucleoside) (entries 7–9). As expected, addition of a base reduced the MIP cleavage from 68% to 18–51%. The relative stability of all four 5′-*O*-MIP 2′-deoxynucleosides (5′-*O*-MIP-T (**1a**), N^4-(2,4-dimethylbenzoyl)-5′-*O*-MIP-2′-deoxycytidine (**2a**), N^6-(2,4-dimethylbenzoyl)-5′-*O*-MIP-2′-deoxyadenosine (**3a**), and N^2-isobutyryl-5′-*O*-MIP-2′-deoxyguanosine (**4a**)) was examined in a mixture of BTT (0.18 mol L^{-1}) and pyridine (25 equiv./nucleoside) (entries 10 and 11). 5′-*O*-MIP-T (**1a**) and 5′-*O*-MIP-dC^{dmb} (**2a**) showed almost equal stability (2–4% MIP cleavage) after 30 min and 60 min time points (corresponding to the total coupling times for 16- and 31-mer oligonucleotides when a 2 min coupling time is used, *cf.* the SPOS experiments below). Slightly lower stability was observed for the purine nucleosides 5′-*O*-MIP-dA^{dmb} (**3a**) and 5′-*O*-MIP-dG^{iBu} (**4a**) (30 min: 5%; 60 min: 10–12% MIP cleavage). The stability of DMT-protected nucleosides follows the same trend. The reason can be attributed to the electronic influence and partial alterations in sugar puckering that can affect protonation of the ether oxygen.

The corresponding stability assessments were conducted with 5′-*O*-DMT-T (entries 1–9). As anticipated, 5′-*O*-DMT exhibited higher stability under the same conditions. Some detritylation was observed under the most acidic conditions, which is consistent with the literature.[31,33]

Stability of 5′-*O*-MIP during oxidation and sulfurization

The stability of 5′-*O*-MIP was examined in the presence of standard oxidation and sulfurization reagents (entries 12–14; Table 1). Exposure to the iodine oxidizing solution (0.05 M; H_2O–pyridine, 1 : 9, v/v) resulted in 18% MIP cleavage after 24 h of incubation (entry 12). Interestingly, only modest stability was observed in the presence of the non-aqueous organic oxidizer (1*S*)-(+)-(10-camphorsulfonyl)-oxaziridine (CSO) (entry 13). Nevertheless, premature MIP cleavage during the oxidation step is not an issue, if acetic anhydride capping is performed before oxidation. MIP remained completely stable in the sulfurization reagent 3-phenyl 1,2,4-dithiazoline-5-one (PolyOrg Sulfa, 0.1 M in acetonitrile) (entry 14).[34]

Optimizing the coupling conditions for the 5′-*O*-MIP building blocks in SPOS

According to the preliminary stability tests described above, 1*H*-tetrazole or BTT with pyridine (or 2,6-lutidine) appeared to be the most suitable conditions to minimize premature MIP cleavage during the coupling. As mentioned above, the synthesizer mixes the phosphoramidite building block (0.1 mol L^{-1} solution, 15 equiv./5′-OH group) and the commercial ready-made activator solution (0.45 mol L^{-1} 1*H*-tetrazole or 0.30 mol L^{-1} BTT in acetonitrile) at a 2 : 3 (v/v) ratio and recycles this combined cocktail through the reaction column at a 4.5 mL min^{-1} flow rate. This refers to 4.5 equiv. of BTT and 6.8 equiv. of 1*H*-tetrazole compared to the building block. Single coupling of each 5′-*O*-MIP building block (**1b–4b**, 15 equiv./5′-OH group) using BTT as the activator (4.5 equiv. of BTT/building block) with a T_6 model sequence on a CPG support (45 μmol g^{-1}; 500 Å) was examined in more detail (Fig. 2). Pyridine was included in the coupling cocktail (the building blocks dissolved in an acetonitrile–pyridine (80 : 20, v/v) solution, corresponding to 25 equiv. of pyridine/building block). A two-minute coupling time with this cocktail, followed by oxidation with 0.05 M iodine in H_2O–pyridine (1 : 9, v/v) solution (12 s at a

5 mL min^{-1} flow rate), afforded quantitatively the desired heptanucleotide products, as verified by UPLC-DAD-ESI-TOF analysis (the 5′-*O*-MIP group was removed, and the released heptanucleotide was analyzed, *cf.* Fig. 3). The coupling time was then extended to 30 and 60 min (simulating 15 and 30 subsequent couplings) to make potential premature MIP cleavage more visible. With pyrimidine building blocks (**1b** and **2b**), 2–4% n + 1 products were formed. With the purine building blocks (**3b** and **4b**), 5–7% n + 1 products were observed (Table 2 and Fig. 3A). The observed amounts of n + 1 side products were consistent with the stability of MIP in the solution (*cf.* Table 1).

To eliminate potential instrument-specific factors, each 5′-*O*-MIP building block (**1b**–**4b**) was also coupled manually to the same T_6-CPG model sequence. The building blocks (0.1 mol L^{-1} in acetonitrile–pyridine (80 : 20, v/v) solution, 15 equiv./5′-OH group) and a ready-made activator solution (0.3 mol L^{-1} BTT in acetonitrile) were mixed at a 2 : 1 (v/v) ratio

Table 2 Automated solid-phase coupling of each 5′-*O*-MIP-protected phosphoramidite building block (**1b**–**4b**) to a T_6-CPG support using 30 and 60 min coupling times. Conditions: **1b**–**4b** (15 equiv./5′-OH-group), BTT (4.5 equiv./**1b**–**4b**) and pyridine (25 equiv./**1b**–**4b**) in acetonitrile at a 4.5 ml min^{-1} flow rate (1 μmol scale). The ratios of the cleaved heptamer product and its n + 1 side-products were determined by UPLC-DAD-ESI-TOF analysis

Coupled amidite	Coupling time (min)	Heptanucleotide product (%)	n + 1 product (%)
1b	30	98	2
1b	60	96	4
2b	30	97	3
2b	60	97	3
3b	30	94	6
3b	60	93	7
4b	30	95	5
4b	60	93	7

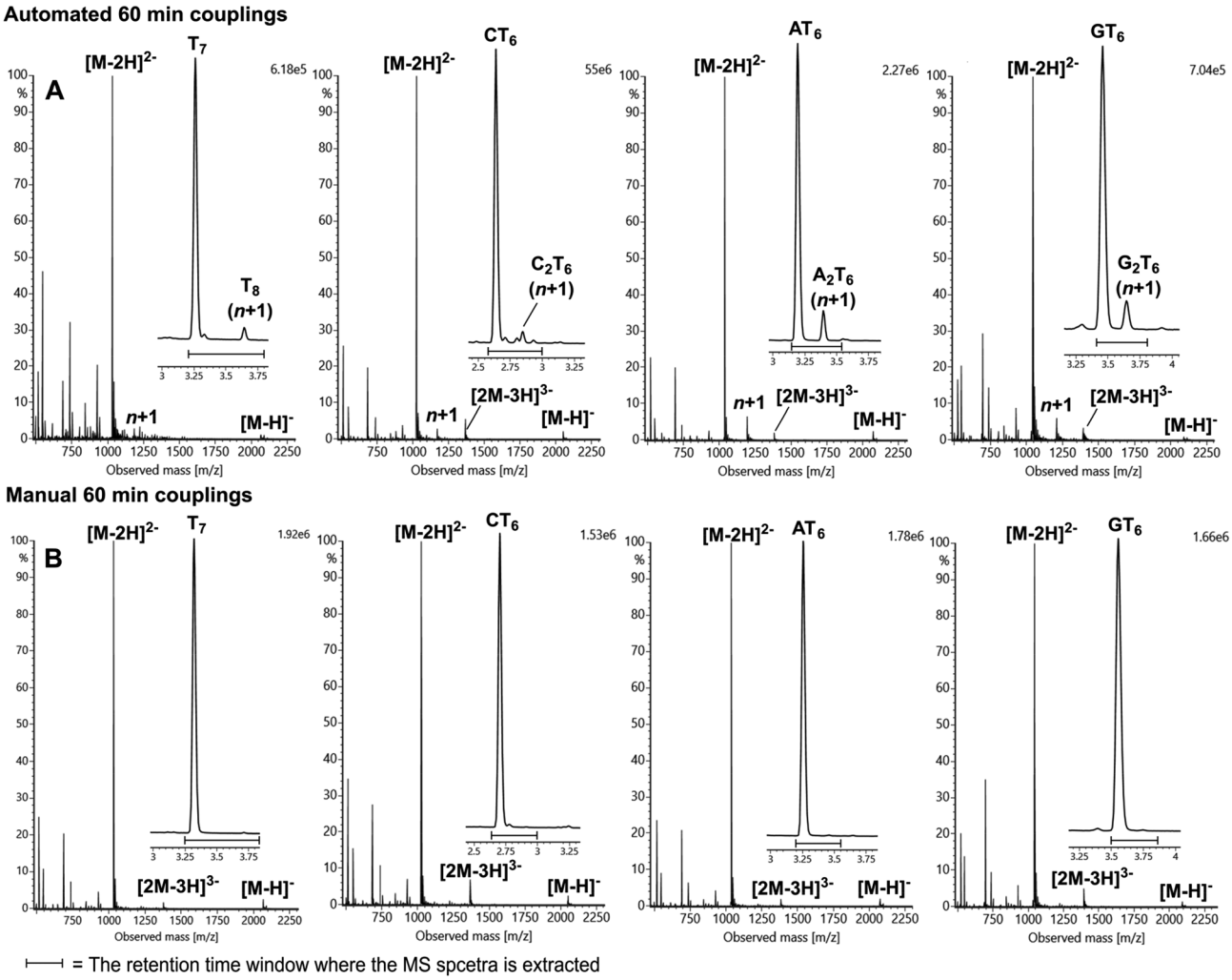

Fig. 3 RP-HPLC chromatograms and MS-spectra of the released crude heptanucleotides, after coupling each 5′-*O*-MIP-protected building block (**1b**–**4b**) to a T_6-CPG support. A = automated couplings at a 4.5 mL min^{-1} flow rate, B = manual couplings in a batch-like vessel. Conditions: **1b**–**4b** (15 equiv./5′-OH group), BTT (4.5 equiv. (A) or 1.5 equiv. (B)/**1b**–**4b**) and pyridine (25 equiv./**1b**–**4b**) in acetonitrile for 60 min (1 μmol scale).

and suspended with the T_6-CPG support under an inert atmosphere on a 1 μmol scale. After coupling, the supports were washed with acetonitrile, followed by oxidation with a mixture of 0.05 M iodine in H_2O–pyridine (1 : 9, v/v). A two-minute coupling time resulted in quantitative coupling of each building block, and gratifyingly, even after an extended 60 min coupling time, no detectable amount of n + 1 products was observed (see Fig. 3B for the UPLC-DAD-ESI-TOF analysis of the released heptanucleotide products).

An 18-mer model oligonucleotide **ON1** (5′-GTT GTA TGA CTT AGT GTA-3′) was next assembled using an automated oligonucleotide synthesizer on a 1 μmol scale. To confirm that all potential failures of the synthesis originated from potential incomplete coupling or premature MIP cleavage, and not from potential failures in the deblocking step, the deblocking time was fixed at 60 s, which was more than sufficient to achieve quantitative removal of the 5′-*O*-MIP group. 1*H*-Tetrazole (6.8 equiv./building block) without added base and BTT (4.5 equiv./building block) with different amounts of pyridine or 2,6-lutidine were tested across a range of coupling times. The target product (**ON1**) was released from the support and analysed by UPLC-DAD-ESI-TOF (Fig. 4). Using 1*H*-tetrazole, a 2 min coupling time was nearly optimal to afford efficient synthesis of **ON1** with only minor amounts of n − 1 and n + 1 side products (Fig. 4A). Shorter coupling times increased the number of n − 1 products (indicating incomplete coupling, *cf.* Fig. S18), whereas longer coupling times led to a higher number of n + 1 products (indicating premature MIP removal, *cf.* Fig. S19). BTT with different concentrations of 2,6-lutidine (pK_a 6.6) led to a weak coupling efficiency even with an extended coupling time (*cf.* Fig. S20). Similarly, BTT (4.5 equiv./building block) with a large excess of pyridine (pK_a 5.2) (building blocks fully dissolved in pyridine, 125 equiv. of pyridine/building block) led to an inadequate coupling efficiency (*cf.* Fig. S21). Reducing the amount of pyridine to 25 equiv. (building blocks dissolved in acetonitrile–pyridine, 80 : 20, v/v) and using a 2 min coupling time yielded a product purity comparable to that obtained with 1*H*-tetrazole (Fig. 4B). The ratio of the activator and the building block solution (acetonitrile–pyridine, 80 : 20, v/v) was also adjusted to a 2 : 1 (v/v) ratio, which reduced molar equivalents of BTT to 1.5 equiv./building block (*cf.* Fig. S23). This mimicked the conditions used for the manual couplings described above (Fig. 3B). However, no reduced amount of the n + 1 products was observed, and based on several replicates, the higher BTT ratio (4.5 equiv./building block) gave a more reproducible result considering the coupling efficiency. In summary, the best results were obtained using 1*H*-tetrazole (6.8 equiv.) without added base or BTT (4.5 equiv.) with pyridine (25 equiv.) for the coupling (*cf.* Fig. S17 and S22). In both cases, a 2 min coupling time can be used for efficient chain elongation of **ON1**, with the purity of the product comparable with respect to n + 1 and n − 1 side products (Fig. 4). The acid potential of 1*H*-tetrazole could be lowered by the added base in a similar manner to that performed with BTT (to further prevent premature MIP removal). However, BTT with pyridine was selected for the subsequent studies because 1*H*-tetrazole is generally avoided in industrial applications due to its hazardous nature. As noticed, the automated synthesis with the 5′-*O*-MIP-protected building blocks **1b–4b** requires careful optimization. Our manual coupling tests, however, verified that the coupling can be performed without notable premature MIP removal even after extended exposure to the activator (Fig. 3B). Therefore, some of the issues are related to the continuous-flow system of the coupling cocktail, in which the conditions (the exposure of the building blocks to the activator) were harder to control compared to the manual coupling. Premature MIP removal could more efficiently be prevented by stirred batch-like reaction conditions on a solid phase. While flow-through SPOS systems seem to be mostly adopted for oligonucleotide manufacturing, a stirred-bed system has been reported to be more suitable for sustainable SPOS.[35]

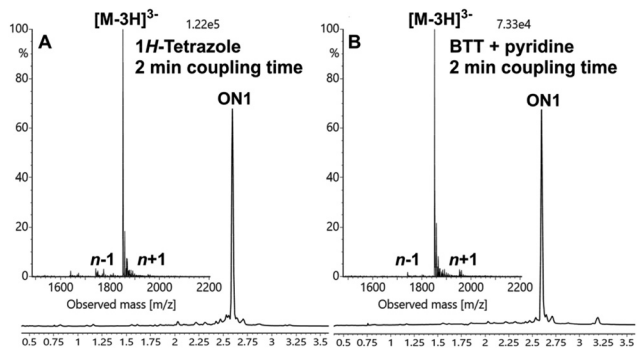

Fig. 4 RP-HPLC profiles and MS-spectra of crude **ON1**, synthesized using the 5′-*O*-MIP-protected building blocks **1b–4b** under optimized coupling conditions. Conditions: coupling (A): **1b–4b** (15 equiv./5′-OH group), 1*H*-tetrazole (6.8 equiv./**1b–4b**), 2 min; oxidation (A): 0.05 M I_2 in H_2O–pyridine (1 : 9, v/v); deblocking (A): DCA in toluene (3 : 97, v/v), 60 s. Coupling (B): **1b–4b** (15 equiv./5′-OH group), BTT (4.5 equiv./**1b–4b**), pyridine (25 equiv./**1b–4b**), 2 min; oxidation (B): same as in (A); deblocking (B): same as in (A). Scale: 1 μmol. See the exact chromatographic conditions in the Experimental section.

Rapid deprotection of 5′-*O*-MIP *vs.* 5′-*O*-DMT

The same model sequence **ON1** was assembled on a 1 μmol scale with an automated oligonucleotide synthesizer using either the 5′-*O*-DMT- or 5′-*O*-MIP-protected phosphoramidite building blocks. The 5′-*O*-MIP-protected building blocks **1b–4b** (0.1 M) were dissolved in acetonitrile–pyridine (80 : 20, v/v), and the 5′-*O*-DMT-protected building blocks (0.1 M) were dissolved in acetonitrile. Syntheses were performed on the same CPG support (45 μmol g^{-1}; 500 Å) using 15 equiv./OH group of the building blocks, BTT as the activator (4.5 equiv. of BTT/building block) and a 2 min coupling time. The oxidation step was performed with a mixture of 0.05 M iodine in H_2O–pyridine (1 : 9, v/v, 12 s at 5 mL min^{-1}). The SPOS conditions for **ON1** are summarized in Table 3. The deblocking time (*i.e.*, 5′-*O*-deprotection) was gradually decreased from 60 s to 15 s to find the minimal acid treatment for the complete removal of the 5′-*O*-MIP and 5′-*O*-DMT groups (the other parameters were

Table 3 Optimized SPOS conditions for **ON1** and **ON2** using the 5′-*O*-MIP and 5′-*O*-DMT building blocks on a 1 μmol scale. Syntheses were performed on a CPG-support (45 μmol/; 500 Å) using 15 equiv. building blocks/5′-OH-group

	Reagent	Time (s)	Volume (mL)	Flow rate (mL min^{-1})
Deblocking MIP	DCA in toluene (3 : 97, v/v)	23	1.5	4
Deblocking DMT	DCA in toluene (3 : 97, v/v)	45	3	4
Coupling	Phosphoramidite building blocks (0.1 M)[a] and BTT (0.3 M) (2 : 3, v/v)	120	0.375	4.5[b]
Oxidation	0.05 M iodine in H_2O–pyridine (1 : 9, v/v)	12	1	5
Sulfurization	0.1 M PolyOrg Sulfa in acetonitrile	150	1.5	0.4
Capping	1-Methylimidazole, acetic anhydride and 2,6-lutidine in acetonitrile (2 : 2 : 3 : 13, v/v/v/v)	12	1.2	6

[a] The 5′-*O*-MIP-building blocks were dissolved in acetonitrile–pyridine, 80 : 20 (v/v) and the 5′-*O*-DMT building blocks in acetonitrile. [b] The coupling cocktail was recycled.

kept constant). A mixture of 3% of dichloroacetic acid in toluene was used for deblocking and delivered to the column at a 4 mL min^{-1} flow rate. Thus, every 15 s of the deblocking refers to the consumption of 1 mL of the reagent. Incomplete 5′-*O*-deprotection can be observed as the formation of deletion sequences (n − 1 products), which were detected by UPLC-DAD-ESI-TOF analysis of the released crude product (Fig. 5). The shortest deblocking time that still yielded a clean product (**ON1**) with DMT protection was 45 s (corresponding to the consumption of 3 mL of the reagent). n − 1 byproducts began to accumulate at deblocking times of ≤30 s, indicating incomplete DMT removal during the synthesis. With the 5′-*O*-MIP-protected building blocks, the deblocking time could be reduced to 23 s (corresponding to the consumption of 1.5 mL of the reagent) without notable accumulation of n − 1 side products. In conclusion, by using the 5′-*O*-MIP-protected building blocks in SPOS, the deblocking time (and the amount of the reagent) could be reduced to approximately half of that needed for the 5′-*O*-DMT-protected building blocks, while still maintaining efficient chain elongation with respect to the formation of n − 1 side products. The relative stability of MIP and DMT has previously been studied in acidic methanol, where deprotection of MIP was 4.5-fold faster compared to the DMT group.[27] The S_N1-type cleavage of MIP and DMT can be sensitive to hydrolytic conditions. Therefore, MeOH (0.1%) as a cation scavenger was also included in the deblocking cocktail, and the syntheses were repeated. However, based on several replicates, no notable difference in deprotection efficiency was observed whether methanol was used or not. Dichloroacetate can act as a sufficient initial scavenger for the released 2-methoxypropan-2-ylium cation in the continuous-flow system of SPOS.

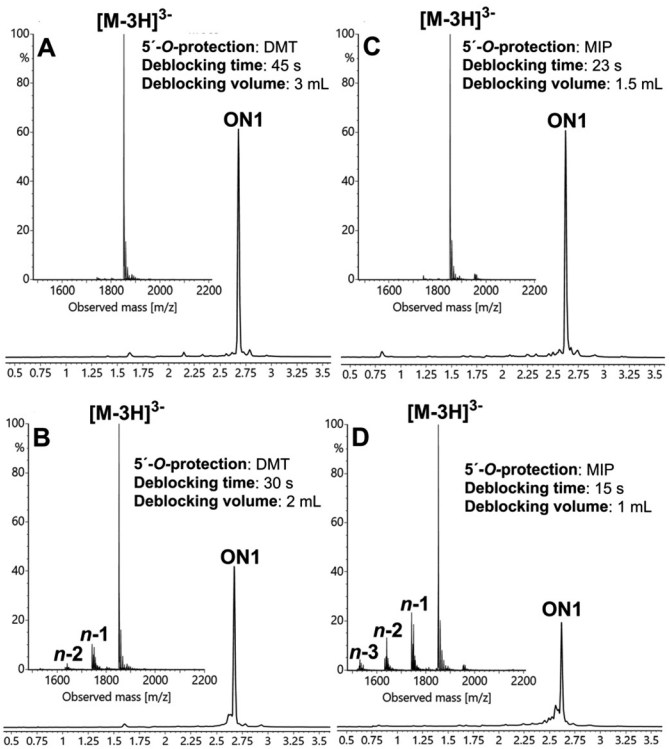

Fig. 5 RP-HPLC chromatograms and MS-spectra of crude **ON1** obtained with different deprotection conditions using either 5′-*O*-DMT- or 5′-*O*-MIP-protected phosphoramidite building blocks **1b–4b**. Conditions: coupling (A and B): 5′-*O*-DMT-protected phosphoramidite building blocks (15 equiv./5′-OH group), BTT (4.5 equiv./building block); oxidation (A and B): 0.05 M I_2 in H_2O–pyridine (1 : 9, v/v), 12 s; deblocking (A and B): DCA in toluene (3 : 97, v/v), 45 s (A) or 30 s (B). Coupling (C and D): **1b–4b** (15 equiv./5′-OH group), BTT (4.5 equiv./building block), pyridine (25 equiv./building block), 2 min; oxidation (C and D): 0.05 M I_2 in H_2O–pyridine (1 : 9, v/v), 12 s; deblocking (C and D): DCA in toluene (3 : 97, v/v), 23 s (C), 15 s (D). Scale: 1 μmol scale. See the exact chromatographic conditions in the Experimental section.

Synthesis of fomivirsen using the 5′-*O*-MIP *vs.* 5′-*O*-DMT building blocks

The performance of the 5′-*O*-MIP protecting group was finally demonstrated in an automated 1 μmol scale synthesis of the therapeutically relevant fomivirsen (**ON2**). This is a 21-mer phosphorothioate oligonucleotide sequence composed of 2′-deoxynucleotides (5′-GCG TTT GCT CTT CTT CTT GCG-3′). As a reference, **ON2** was synthesized using the 5′-*O*-DMT building blocks (15 equiv./5′-OH group, 4.5 equiv. of BTT/building block, 2 min coupling time, and a 45 s detritylation time = 3 mL of deblocking reagent consumption, *cf.* Table 3). Sulfurization was performed using 0.1 M PolyOrg Sulfa in acetonitrile (2.5 min at 0.4 mL min^{-1}). UPLC-DAD-ESI-TOF analysis of the released crude product (**ON2**) mixture using the 5′-*O*-DMT-building blocks is shown in Fig. 6A. The crude yield

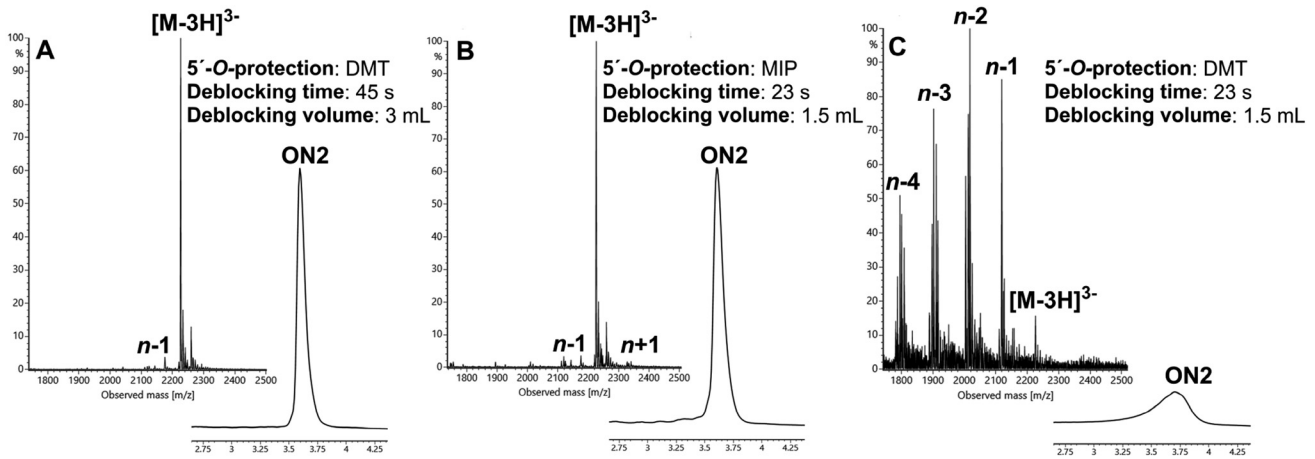

Fig. 6 Comparison of the RP-HPLC chromatograms and MS-spectra of crude **ON2**. Optimized conditions were used for the 5′-*O*-DMT- and 5′-*O*-MIP-protecting group strategies (A and B). For the 5′-*O*-MIP protecting group, the optimized deprotecting conditions were applied for the 5′-*O*-DMT building blocks (C). Conditions: coupling (A): 5′-*O*-DMT-protected phosphoramidite building blocks (15 equiv./5′-OH group), BTT (4.5 equiv./building block), 2 min; sulfurization (A): 0.1 M PolyOrg Sulfa in acetonitrile, 2.5 min; deblocking (A): DCA in toluene (3 : 97, v/v), 45 s (1 μmol scale). Coupling (B): **1b–4b** (15 equiv./5′-OH group), BTT (4.5 equiv./**1b–4b**), pyridine (25 equiv./**1b–4b**), 2 min; sulfurization (B): same as in (A); deblocking (B): DCA in toluene (3 : 97, v/v), 23 s (1 μmol scale). Coupling (C): 5′-*O*-DMT-protected phosphoramidite building blocks (15 equiv./5′-OH group), BTT (4.5 equiv./building block), 2 min; sulfurization (C): same as in (A); (C) deblocking: same as in (B) (1 μmol scale). See the exact chromatographic conditions in the Experimental section.

of **ON2** was 85% based on the UV absorbance. The 5′-*O*-MIP-building blocks (**1b–4b**) were dissolved in acetonitrile–pyridine (80 : 20, v/v) solution (25 equiv. of pyridine/building block) and used for the assembly of **ON2**, following the coupling and deblocking conditions optimized above: BTT (4.5 equiv./building block) with a 2 min coupling time and 23 s deblocking treatment (=1.5 mL consumption of the reagent, *cf.* Table 3). UPLC-DAD-ESI-TOF analysis of the released crude product (**ON2**) mixture using the 5′-*O*-MIP-building blocks is shown in Fig. 6B. The crude yield of **ON2** was 81%, which is comparable to the previous **ON2** synthesis using the 5′-*O*-DMT-building blocks. As shown, nearly similar product (**ON2**) purity can be obtained, whether **ON2** was synthesized using the 5′-*O*-DMT or MIP building blocks (Fig. 6A *vs.* B). A tiny amount of $n + 1$ and $n - 1$ by-products can be observed using the 5′-*O*-MIP-building blocks. **ON2** synthesis was repeated using the 5′-*O*-DMT building blocks but using the shorter (23 s) deblocking treatment that was sufficient for the deprotection of the MIP group. UPLC-DAD-ESI-TOF analysis of the released crude product mixture is shown in Fig. 6C. Only a small amount of **ON2** and a number of shorter sequences can be observed. Therefore, application of the 5′-*O*-MIP protecting group strategy reduced the total deblocking reagent consumption in **ON2** synthesis from 63 mL to 33 mL. Consequently, the proportion of the deblocking reagent within the total waste stream decreased from 21% to 12%, corresponding to an overall waste reduction of approximately 10% at this scale.

Deblocking waste analysis

During the detritylation step, the DMT group is released into the deblocking waste stream as a cation, which then reacts with available scavengers (counterions of the acid or residual water). The release of DMT results in about 35% loss of molecular weight during each addition of the monomer, which is economically and environmentally impractical for commercial-scale manufacturing of therapeutic oligonucleotides to treat large patient populations. Although strategies for recycling and reusing the DMT group have been proposed, they have not yet been implemented on an industrial scale in oligonucleotide manufacturing.[36] To assess the environmental impact of the MIP protecting group, the corresponding deblocking waste stream was analyzed. MIP was removed using DCA in toluene-d_8 (3 : 97, v/v), and the resulting waste mixture was collected and characterized by ^{1}H NMR spectroscopy (*cf.* Fig. S35). As expected, only acetone and methanol were detected in the spectra. The released 2-methoxypropan-2-ylium cation can initially react with the dichloroacetate ion (can also convert back to 2-methoxypropene) and then react with water residues in the deblocking solution, which yields acetone and methanol. This clean waste stream could potentially be reused for 5′-*O*-MIP deblocking over several cycles in the synthesizer.

Conclusions

The applicability of 5′-*O*-MIP protection in automated SPOS of 18- and 21-mer 2′-deoxyribonucleotides, including a therapeutically relevant phosphorothioate sequence (fomivirsen), has been accomplished successfully. The pros, cons, and future applications of the 5′-*O*-MIP-protecting group in SPOS are summarized in Table 4. By using the 5′-*O*-MIP-protected building blocks, the deblocking time (and the amount of the deblocking reagent) could be reduced to half of that needed

Table 4 Pros and cons of the 5′-*O*-MIP-protected building blocks in SPOS

Pros
• Straightforward and efficient synthesis of the 5′-*O*-MIP-protected nucleosides[30] • The phosphoramidite building blocks of MIP exhibit good atom economy, are amorphous free-flowing solids and are soluble in acetonitrile[30] • The fast deprotection rate of MIP can lower the overall PMI of oligonucleotide synthesis and reduce undesired depurination • The deblocking waste solution of MIP contains volatile small-molecule by-products (acetone and methanol), which may facilitate recycling and reuse during large-scale production
Cons
• The deblocking step cannot be colorimetrically detected as in the DMT group • The sensitivity to premature 5′-*O*-MIP-cleavage limits the use of a strongly acidic activator
Future directions
• The scalability of the SPOS and the compatibility of the building blocks for siRNA synthesis should be examined • Further optimization of MIP-cleavage for the synthesis of purine-rich long DNA sequences • Adoption of alternative coupling chemistry with MIP, especially the advanced P(v) chemistry that operates under basic conditions, should be examined in SPOS[26,37–39] • A protocol for detection methods for the released acetone could be integrated into the automated synthesizer

for the standard 5′-*O*-DMT-protected building blocks. Furthermore, the relatively clean waste stream of the deprotection, which consisted of acetone and methanol, may open new opportunities for waste recycling and reuse. The detritylation cycle is one of the highest PMI contributing steps in the upstream process of SPOS.[3] If the 5′-*O*-MIP-protecting group can be implemented in large-scale production, the overall PMI of the manufacturing process would be reduced by approximately 10%, representing a marked improvement in process sustainability. The by-products of the MIP deprotection are not chromophores. This is a shortcoming that does not allow real-time spectrophotometric monitoring of deprotection. However, this is not a serious issue for process optimization, in which alternative detection methods for the released acetone can be applied and integrated into the synthesizer.

This study clearly demonstrated the assembly of 18- and 21-mer 2′-deoxyribonucleotide sequences on a laboratory scale (1 μmol). The scalability of the SPOS, the alternative instrumentation (*e.g.*, stirred-bed reactor), and the wider application of 5′-*O*-MIP protection for the assembly of 2′-modified ribonucleotides, with more demanding coupling conditions, should be examined. A milder phosphoramidite coupling protocol using BTT as the activator in a mixture of pyridine and acetonitrile has been developed to prevent premature 5′-*O*-MIP cleavage. This required careful optimization to balance the coupling efficiency of the building blocks and simultaneously prevent the premature MIP cleavage. It is likely that the acid sensitivity of MIP protection may require the use of alternative mildly acidic activators. This would encourage the use of alternative coupling chemistry with 5′-*O*-MIP protection. Recent achievements in pentavalent phosphorus have shown that the (P(v)) coupling chemistry can be equally efficient as the phosphoramidite (P(III)) coupling chemistry in SPOS.[37–39] The reaction conditions in the P(v) coupling are basic, which works well with 5′-*O*-MIP-protection, as already demonstrated in a liquid-phase approach.[26]

Experimental

General information

NMR spectra were recorded on a Bruker Avance 500 MHz instrument and mass spectra on a Waters RDa UPLC-DAD-ESI-TOF system. Oligonucleotides were analyzed using an ACQUITY Premier BEH C18 column (2.1 × 50 mm, 1.7 μm, detection at λ = 260 nm, flow rate = 0.4 mL min^{-1} and column temperature = 60 °C). Gradient elution of MeOH (**ON1** and **ON2**: 5–25%, T_7, CT_6, AT_6: 5–13%, GT_6: 5–9%) in a mixture of aqueous hexafluoroisopropanol (40 mM) and triethylamine (7 mM) over 4 min was performed. A Thermo ODS Hypersil C_{18} column (4.6 × 250 mm, 5 μm, detection at λ = 260 nm and flow rate = 1.0 mL min^{-1}) and gradient elution of acetonitrile in aqueous 50 mM triethylammonium acetate (TEAA) were employed for the RP-HPLC analysis of 5′-*O*-protected nucleosides. Gradient for 5′-*O*-MIP-T: 10–55% of acetonitrile over 20 min, and for 5′-*O*-DMT-T: isocratic hold at 10% over 2 min and 10–100% of acetonitrile over 18 min. Gradient for 5′-*O*-MIP-dC^{dmbz}, 5′-*O*-MIP-dA^{dmbz}, and 5′-*O*-MIP-dG^{iBu}: 10–17% of acetonitrile over 10 min and 17–100% over 10 min.

Synthesis of 5′-*O*-MIP-protected nucleosides and phosphoramidite building blocks

The synthesis procedures for 5′-*O*-MIP-T (**1a**),[24,30] 5′-*O*-dC^{dmb} (**2a**),[25] 5′-*O*-dA^{dmb} (**3a**),[24] and 5′-*O*-MIP-dG^{iBu} (**4a**)[26,30] nucleosides and 5′-*O*-MIP-T (**1b**),[24,30] 5′-*O*-dC^{dmb} (**2b**),[25] 5′-*O*-dA^{dmb} (**3b**),[25] and 5′-*O*-MIP-dG^{iBu} (**4b**)[24,30] 3′-*O*-phosphoramidite building blocks are previously published.

Stability study of 5′-*O*-MIP- and 5′-*O*-DMT-protected nucleosides under different conditions (Table 1)

The 5′-*O*-protected nucleosides were dried with P_2O_5 overnight and dissolved under the given conditions: (entry 1) **1a** or 5′-*O*-DMT-T (0.11 mol L^{-1}), BTT (0.11 mol L^{-1}), acetonitrile–DMF (1 : 1, v/v); (entry 2) **1a** or 5′-*O*-DMT-T (0.11 mol L^{-1}), 1*H*-tetrazole (0.11 mol L^{-1}), acetonitrile–DMF (1 : 1, v/v); (entry 3) **1a** or

5′-*O*-DMT-T (0.11 mol L^{-1}), DCI (0.11 mol L^{-1}), acetonitrile–DMF (1 : 1, v/v); (entry 4) **1a** or 5′-*O*-DMT-T (0.11 mol L^{-1}), PTFA/NMI (0.11 mol L^{-1}/0.05 mol L^{-1}), acetonitrile–DMF (1 : 1, v/v); (entry 5) **1a** or 5′-*O*-DMT-T (0.04 mol L^{-1}), BTT (0.18 mol L^{-1}), acetonitrile–DMF (9 : 1, v/v); (entry 6) **1a** or 5′-*O*-DMT-T (0.04 mol L^{-1}), 1*H*-tetrazole (0.27 mol L^{-1}), acetonitrile–DMF (9 : 1, v/v); (entry 7) **1a** or 5′-*O*-DMT-T (0.04 mol L^{-1}), BTT (0.18 mol L^{-1}), acetonitrile–DMF–pyridine (41 : 5 : 4, v/v/v); (entry 8) **1a** or 5′-*O*-DMT-T (0.04 mol L^{-1}), BTT (0.18 mol L^{-1}) acetonitrile–pyridine (3 : 2, v/v); (entry 9) **1a** or 5′-*O*-DMT-T (0.04 mol L^{-1}), BTT (0.18 mol L^{-1}), acetonitrile–DMF–2,6-lutidine (41 : 5 : 4, v/v/v) (entries 10 and 11) **1a**, **2a**, **3a** or **4a** (0.04 mol L^{-1}), BTT (0.18 mol L^{-1}), acetonitrile–DMF–pyridine (41 : 5 : 4, v/v/v); (entry 12) **1a** or 5′-*O*-DMT-T (0.06 mol L^{-1}), I_2 oxidizer (0.05 mol L^{-1} in H_2O–pyridine, 9 : 1, v/v); (entry 13) **1a** or 5′-*O*-DMT-T (0.05 mol L^{-1}), CSO (0.42 mol L^{-1}), acetonitrile–DMF (5 : 1, v/v); (entry 14) **1a** or 5′-*O*-DMT-T (0.05 mol L^{-1}), PolyOrg Sulfa (0.08 mol L^{-1}) acetonitrile–DMF (5 : 1, v/v). Methanol was added to all reactions (2 equiv./nucleoside). The reaction mixtures were shaken and monitored by RP-HPLC after 30 min and 60 min (entries 10 and 11) or 24 h (entries 1–9 and 12–14).

Optimized conditions for automated solid-phase oligonucleotide synthesis and product analysis (Tables 2 and 3)

Oligonucleotides were synthesized on an ÄKTA OligoPilot™ Plus 10 automated synthesizer on a 1 μmol scale using a pre-loaded long-chain alkyl-amino CPG (45 μmol g^{-1}, 500 Å) support. Phosphoramidites (15 equiv./5′-OH-group) were used as 0.1 M solutions. The 5′-*O*-DMT building blocks were dissolved in acetonitrile and the 5′-*O*-MIP building blocks (**1b–4b**) in acetonitrile–pyridine (80 : 20, v/v). BTT (0.3 M in acetonitrile) was used as the activator. For the coupling, a 2 : 3 (v/v) mixture of the phosphoramidite building block and activator solution was recycled through the synthesis column at a flow rate of 4.5 mL min^{-1} for 2 min. For the oxidation and sulfurization, respectively, a mixture of 0.05 M iodine in H_2O–pyridine (1 : 9, v/v) (12 s at a flow rate of 5 mL min^{-1}) and 0.1 M PolyOrg Sulfa in acetonitrile (2.5 min at a flow rate of 0.4 mL min^{-1}) was used. For the capping, a mixture of 1-methylimidazole, acetic anhydride and 2,6-lutidine in acetonitrile (2 : 2 : 3 : 13, v/v/v/v, 12 s at a flow rate of 6 mL min^{-1}) was used. For the deblocking, a mixture of DCA in toluene (3 : 97, v/v, at a 4 mL min^{-1} flow rate) was used. The deblocking times for the 5′-*O*-MIP and 5′-*O*-DMT building blocks were 23 s and 45 s, respectively. 25% aqueous ammonia at 55 °C was used for the deprotection/release of the oligonucleotides. The crude product mixtures were analyzed by UPLC-DAD-ESI-TOF.

Extended couplings to T_6-CPG in an automated synthesizer using 5′-*O*-MIP-protected phosphoramidite building blocks

Each 5′-*O*-MIP-protected phosphoramidite building block (**1b–4b**) was coupled to T_6-CPG (45 μmol g^{-1}, 500 Å, 1 μmol) using 30 min and 60 min coupling times. Otherwise, the protocol above for automated SPOS was applied.

Manual couplings to T_6-CPG using 5′-*O*-MIP-protected phosphoramidite building blocks

Each 5′-*O*-MIP-protected phosphoramidite building block (**1b–4b**) was manually coupled to T_6-CPG (45 μmol g^{-1}, 500 Å, 1 μmol) using 2 min and 60 min coupling times. T_6-CPG, BTT (0.3 M in acetonitrile, 75 μL) and phosphoramidite solution (0.1 M in acetonitrile–pyridine, 80 : 20, v/v, 150 μL) were combined in a vial under a nitrogen atmosphere. After coupling, the mixture was transferred to a synthesis column and washed with acetonitrile. Oxidation was performed using a mixture of 0.05 M iodine in H_2O–pyridine (1 : 9, v/v, 2 min) followed by an acetonitrile wash. The 5′-*O*-MIP group was removed using a mixture of DCA in toluene (3 : 97, v/v, 2 min), followed by an acetonitrile wash. The heptanucleotide products were released using 25% aqueous ammonia at 55 °C, and the product mixture was analyzed by UPLC-DAD-ESI-TOF.

Author contributions

VS: data curation, investigation, validation, visualization, and writing – original draft; MO: conceptualization, supervision, and writing – review & editing; AGM: conceptualization and writing – review & editing; AH: conceptualization and writing – review & editing; YSS: conceptualization and writing – review & editing; PV: conceptualization, project administration, supervision, and writing – review & editing.

Conflicts of interest

There are no conflicts to declare.

Data availability

Data for this article, including chromatograms and MS-spectra, are available in the supplementary information (SI). Supplementary information is available. See DOI: https://doi.org/10.1039/d6ob00858e.

Acknowledgements

Financial support from the Doctoral Programme in Exact Sciences (EXACTUS) is acknowledged.

References

1 S. L. Beaucage and M. H. Caruthers, *Tetrahedron Lett.*, 1981, **22**, 1859–1862.
2 *Sustainability in TIDES chemistry: green approaches to oligonucleotides and oligopeptides synthesis*, ed. A. Tolomelli, L. Ferrazzano and W. Cabri, Royal Society of Chemistry, Cambridge, 2024.

3 B. I. Andrews, F. D. Antia, S. B. Brueggemeier, L. J. Diorazio, S. G. Koenig, M. E. Kopach, H. Lee, M. Olbrich and A. L. Watson, *J. Org. Chem.*, 2021, **86**, 49–61.
4 Y. S. Sanghvi, V. T. Ravikumar, A. N. Scozzari and D. L. Cole, *Pure Appl. Chem.*, 2001, **73**, 175–180.
5 L. Ferrazzano, D. Corbisiero, A. Tolomelli and W. Cabri, *Green Chem.*, 2023, **25**, 1217–1236.
6 J. B. Chattopadhyaya and C. B. Reese, *J. Chem. Soc., Chem. Commun.*, 1978, 639–640.
7 P. R. J. Gaffney, L. Changsheng, M. V. Rao, C. B. Reese and J. G. Ward, *J. Chem. Soc., Perkin Trans. 1*, 1991, 1355–1360.
8 M. P. Coleman and M. K. Boyd, *Tetrahedron Lett.*, 1999, **40**, 7911–7915.
9 M. P. Coleman and M. K. Boyd, *J. Org. Chem.*, 2002, **67**, 7641–7648.
10 R. P. Samudrala, S. Penjarla, R. Gundla and B. Purna Chandra Rao, *Tetrahedron Lett.*, 2023, **121**, 154480.
11 S. A. Scaringe, F. E. Wincott and M. H. Caruthers, *J. Am. Chem. Soc.*, 1998, **120**, 11820–11821.
12 I. Hirao, M. Koizumi, Y. Ishido and A. Andrus, *Tetrahedron Lett.*, 1998, **39**, 2989–2992.
13 S. A. Scaringe, *Methods*, 2001, **23**, 206–217.
14 K. Kamaike, H. Takahashi, T. Kakinuma, K. Morohoshi and Y. Ishido, *Tetrahedron Lett.*, 1997, **38**, 6857–6860.
15 H. Seliger and U. Kotschi, *Nucleosides Nucleotides*, 1985, **4**, 153–155.
16 C. Lehman, Y.-Z. Xu, C. Christodoulou, Z. Tan and M. J. Gait, *Nucleic Acids Res.*, 1989, **17**, 2379–2390.
17 A. C. Pease, D. Solas, E. J. Sullivan, M. T. Cronin, C. P. Holmes and S. P. Fodor, *Proc. Natl. Acad. Sci. U. S. A.*, 1994, **91**, 5022–5026.
18 M. C. Pirrung and J.-C. Bradley, *J. Org. Chem.*, 1995, **60**, 1116–1117.
19 A. Hasan, K.-P. Stengele, H. Giegrich, P. Cornwell, K. R. Isham, R. A. Sachleben, W. Pfleiderer and R. S. Foote, *Tetrahedron*, 1997, **53**, 4247–4264.
20 N. Kretschy, A.-K. Holik, V. Somoza, K.-P. Stengele and M. M. Somoza, *Angew. Chem., Int. Ed.*, 2015, **54**, 8555–8559.
21 H. Seliger, *Curr. Protoc. Nucleic Acid Chem.*, 2000, 2.3.1–2.3.34.
22 H. Seliger and Y. S. Sanghvi, *Curr. Protoc.*, 2024, **4**, e999.
23 A. G. Molina, A. M. Jabgunde, P. Virta and H. Lönnberg, *Beilstein J. Org. Chem.*, 2014, **10**, 2279–2285.
24 A. G. Molina, V. Kungurtsev, P. Virta and H. Lönnberg, *Molecules*, 2012, **17**, 12102–12120.
25 P. Rosenqvist, V. Saari, M. Ora, A. G. Molina, A. Horvath and P. Virta, *J. Org. Chem.*, 2024, **89**, 13005–13015.
26 P. Rosenqvist, V. Saari, E. Pajuniemi, A. Gimenez Molina, M. Ora, A. Horvath and P. Virta, *J. Org. Chem.*, 2023, **88**, 10156–10163.
27 Z. Liang, P. Rosenqvist, E. Pajuniemi, M. Ora, P. Heinonen, P. Virta and M. Oivanen, *Eur. J. Org. Chem.*, 2023, **26**, e202300614.
28 J. Marlyn, A. Arora and M. J. Damha, *Org. Lett.*, 2026, **28**, 6889–6893.
29 Z. Liang, H. Koivikko, M. Oivanen and P. Heinonen, *Beilstein J. Org. Chem.*, 2019, **15**, 746–751.
30 V. Saari, A. Eerola, M. Ora, A. Gimenez Molina, A. Horvath, Y. S. Sanghvi and P. Virta, *Org. Lett.*, 2025, **27**, 8251–8256.
31 A. Eleuteri, D. C. Capaldi, A. H. Krotz, D. L. Cole and V. T. Ravikumar, *Org. Process Res. Dev.*, 2000, **4**, 182–189.
32 R. Wörl and H. Köster, *Tetrahedron*, 1999, **55**, 2957–2972.
33 A. Schwenger, N. Birchall and C. Richert, *Eur. J. Org. Chem.*, 2017, **2017**, 5852–5864.
34 S. K. Roy and J.-Y. Tang, *United States Pat*, US6500944B2, 2002.
35 D. Samson and M. Marco, *Improving Oligonucleotide Manufacture with Stirred-Bed Technology, [White paper]*, BACHEM, 2023.
36 Z. Guo, H. M. Pfundheller and Y. S. Sanghvi, *Org. Process Res. Dev.*, 1998, **2**, 415–417.
37 K. W. Knouse, J. N. deGruyter, M. A. Schmidt, B. Zheng, J. C. Vantourout, C. Kingston, S. E. Mercer, I. M. Mcdonald, R. E. Olson, Y. Zhu, C. Hang, J. Zhu, C. Yuan, Q. Wang, P. Park, M. D. Eastgate and P. S. Baran, *Science*, 2018, **361**, 1234–1238.
38 Y. Huang, K. W. Knouse, S. Qiu, W. Hao, N. M. Padial, J. C. Vantourout, B. Zheng, S. E. Mercer, J. Lopez-Ogalla, R. Narayan, R. E. Olson, D. G. Blackmond, M. D. Eastgate, M. A. Schmidt, I. M. McDonald and P. S. Baran, *Science*, 2021, **373**, 1265–1270.
39 M. Nassir, L. Gherardi, R. L. Redman, Y. Jin, F. Yao, Y. Yang, N. Raheja, A. Natarajan, D. Butler, K. W. Knouse and P. S. Baran, *Org. Lett.*, 2025, **27**, 97–102.